An *in ovo* investigation into the hepatotoxicity of cadmium and chromium evaluated with light- and transmission electron microscopy and electron energy-loss spectroscopy

Chantelle Venter[1], Hester M. Oberholzer[1], Helena Taute[1], Franscious R. Cummings[2] and Megan J. Bester[1]

[1]*Department of Anatomy, Faculty of Health Sciences, University of Pretoria, Pretoria, South Africa*
[2]*Electron Microscope Unit, University of the Western Cape, Bellville, South Africa*

Address correspondence to Hester M. Oberholzer, Department of Anatomy, Faculty of Health Sciences, University of Pretoria, Pretoria 0001, South Africa; E-mail: nanette.oberholzer@up.ac.za

Excessive agriculture, transport and mining often lead to the contamination of valuable water resources. Communities using this water for drinking, washing, bathing and the irrigation of crops are continuously being exposed to these heavy metals. The most vulnerable is the developing fetus. Cadmium (Cd) and chrome (Cr) were identified as two of the most prevalent heavy metal water contaminants in South Africa. In this study, chicken embryos at the stage of early organogenesis were exposed to a single dosage of 0.430 μM physiological dosage (PD) and 430 μM (×1000 PD) $CdCl_2$, as well as 0.476 μM (PD) and 746 μM (×1000 PD) $K_2Cr_2O_7$. At day 14, when all organ systems were completely developed, the embryos were terminated and the effect of these metals on liver tissue and cellular morphology was determined with light- and transmission electron microscopy (TEM). The intracellular localization of these metals was determined using electron energy-loss spectroscopy (EELS). With light microscopy, the PD of both Cd and Cr had no effect on liver tissue or cellular morphology. At ×1000 PD both Cd and Cr caused sinusoid dilation and tissue necrosis. With TEM analysis, Cd exposed hepatocytes presented with irregular chromatin condensation, ruptured cellular membranes and damaged or absent organelles. In contrast Cr caused only slight mitochondrial damage. EELS revealed the bio-accumulation of Cd and Cr along the cristae of the mitochondria and chromatin of the nuclei.

Keywords: Cadmium, chromium, liver, mitochondria, electron energy-loss spectroscopy.

Introduction

Many heavy metals are essential for human biological functions and occur as structural elements, stabilizers of biological structures, components of control mechanisms like nerves and muscles, as well as components of redox systems.[1] However, some heavy metals, especially at high concentrations, can have toxic, carcinogenic and/or teratogenic effects. The main anthropogenic sources of human exposure to heavy metals are through agriculture, transport, mining and related operations. These activities are also the main sources of increased environmental heavy metal levels.[2]

Communities living in these regions that use contaminated water are the most vulnerable, especially children and pregnant woman, with the developing fetus being at risk. This water is used for drinking, preparing food, and bathing, as well as the irrigation of crops. Heavy metals are absorbed through the skin, by inhalation or orally [3] and the degree of heavy metal toxicity depends on the dose, duration, route of administration and other physio-logical factors, especially nutrition.[2,4] In the USA there is a lack of international standards for safe threshold levels for cadmium (Cd) especially related to pregnancy.[5] Like-wise no information is available for other metals such as chromium (Cr) found in South Africa. The high rate of cellular division and differentiation of embryological cells and tissue makes the fetus highly vulnerable to the toxic effects of heavy metals.[5]

In South Africa the mining sector is estimated to be the fifth largest in the world and the largest reserve of manganese and platinum group metals worldwide is found within the country. South Africa also has one of the largest reserves of gold, diamond, chromium ore and vanadium.[6] When heavy metals from these mines are not correctly disposed of, heavy metal pollution is the consequential result. Several studies have shown that levels of these metals, especially chromium, lead, zinc, titanium, manganese,

strontium, copper and tin, are increased in various water sources.[7,8]

In the current study, two heavy metals, Cd and Cr, were identified based on the risk of exposure in South Africa during pregnancy.[9–11] In addition, both metals cross the placenta and the liver has been found to be a major site of Cd and Cr bio-accumulation.[12–14] The effect of these metals on the embryological cellular structure of the liver was evaluated using an *in ovo* chick model. In conjunction with the histological and ultrastructural evaluation, electron energy-loss spectroscopy (EELS) was used to analyse the possible presence and location of the heavy metals in the liver tissue.

Materials and methods

Obtaining fertilized eggs

Ethical clearance for the use of chicken embryos for experimental purposes was obtained from the Animal Ethics Committee (AEC) of the University of Pretoria (h006-13), South Africa. Fertilized broiler hatching eggs were obtained from a local farmer in the Bronkhorstspruit district in Gauteng, South Africa. A total number of 75 eggs were used (15 eggs per group) and the eggs were incubated at 37°C for two days before exposure.

Exposure

On the third embryonic day, a hole was drilled into the blunt end (air chamber) of the egg under aseptic conditions. The relevant concentrations of the control and experimental groups were injected into the eggs through the air sac onto the chorioallantoic membrane (CAM) using a calibrated micropipette. The four experimental groups were exposed to different concentrations of the two heavy metals used in this study as indicated in Table 1. The heavy metals were administered as $CdCl_2$ [Merck (Pty) Ltd, South Africa] and $K_2Cr_2O_7$ [Merck (Pty) Ltd, South Africa] at physiological dose (PD), ×1000 PD dissolved in sterile water.

The Cd and Cr concentrations were calculated according to the human physiological dose (Cd: 30 μg[15] and Cr: 284.28 μg[16]) and subsequently downscaled to be at the physiologically appropriate concentration for the embryos. After the heavy metal administration, the holes were sealed with paraffin wax and were then returned to the incubator for 11 days.

Table 1. Control and experimental group dosages.

Group	*Exposure (μM metal ion)*
Control	ddH_2O
Cd PD	0.430 μM
Cd ×1000 PD	430 μM
Cr PD	0.476 μM
Cr ×1000 PD	476 μM

Termination

On day 14, the embryos were terminated, liver tissue harvested and cut into 1 mm^3 for transmission electron microscopy with the remainder of the sample processed for light microscopy.

Light microscopy tissue processing

The liver samples were fixed in a 2.5% glutaraldehyde (GA)/formaldehyde (FA) in 0.075M sodium phosphate (Na_3PO_4) buffer (pH = 7.4) solution and dehydrated in 30%, 50%, 70%, 90% and three changes of 100% ethanol. The samples were cleared with xylene (Sigma-Aldrich, South Africa), embedded in paraffin wax (Sigma-Aldrich) and 3–5 μm sections were made with a Leica RM 2255 wax microtome (Leica Biosystems GmbH Nussloch, Germany). Tissue sections were stained with haematoxylin and eosin (H&E) to evaluate general tissue morphology with a Nikon Optiphod transmitted light microscope (New York, NY, USA). Three samples were randomly selected from each group for light microscopy analysis.

Transmission electron microscopy tissue processing

The liver samples were fixed in 2.5% GA/FA in 0.075M PO_4 buffer (pH = 7.4), rinsed three times in 0.075M PO_4 buffer before it was placed in the secondary fixative, 1% osmium tetroxide solution for 1 h. Following secondary fixation, the samples were rinsed again as described above. The samples were then dehydrated in 30%, 50%, 70%, 90% and three changes of 100% ethanol. All reagents were obtained from Sigma-Aldrich, South Africa. The samples were embedded in EMbed resin (SPI supplies, West Chester, PA, USA) and ultra-thin sections (70–100 nm) were cut with a diamond knife using an ultramicrotome (Leica Biosystems GmbH). Samples were then contrasted with uranyl acetate and lead citrate, after which they were examined with a JEOL transmission electron microscope (TEM) (JEM 2100F, Tokyo, Japan). Three samples were randomly selected from each group for TEM analysis.

Electron energy-loss spectroscopy measurements

The Tecnai F20 high resolution TEM (200 kV, FEI, Hillsboro, OR, USA) equipped with the GIF 2001 energy filter for electron energy-loss spectroscopy (EELS) and electron spectral imaging (ESI) analyses was used to evaluate ±60 nm thick liver sections. When an unidentified electron-dense granule or cluster of electron-dense granules was observed in the tissue with TEM, the EELS was used to determine if these clusters contained the heavy metals

under investigation. The results were displayed as an EELS spectrum, confirming the presence of the heavy metals in the sample. Together with the ESI color map of the specific area analyzed, the exact position of the metals in the sample was visually expressed.

Due to the low energy-loss signals of the different metals, the EELS spectra were collected in normal parallel beam TEM mode, without an objective aperture and employing a GIF entrance aperture of 3 mm. This allowed for the use of a large collection semi-angle, $\beta \sim 100$ mrad, which greatly improved the signal-to-noise ratio of the spectra. To remove the effects of plural scattering and the contribution from low energy plasmon losses, each spectrum was background subtracted using a power law lineshape. This was followed by further deconvoluting the ionization edges using a Log-Fourier iterative process, as to remove all other plural scattering contribution.

The ESI maps were collected using the Gatan 3 window method with an energy slit width of 20 eV. For construction of the Cr map, the pre-edge 1 and pre-edge 2 energy windows were centered at 515 and 550 eV, respectively, whereas the post-edge window was centered at 583 eV so as to coincide with the onset of the Cr $L_{2,3}$ ionization edge at 573 eV. The positions of the pre-edge 1 and 2 windows were based on the background subtraction model obtained from the EELS analyses when using 2 energy windows. This ensured that only energy loss contributions from the metal under investigation were mapped. Similarly, for mapping of the energy-loss contributions of Cd, the pre-edge 1 and 2 windows were placed at 374 and 394 eV, with a post-edge onset centered at 414 eV.

Results

In Figures 1A and B the normal embryonic histology of the liver can be seen with multi-cellular layered plates of hepatocytes (white arrows), and normally spaced

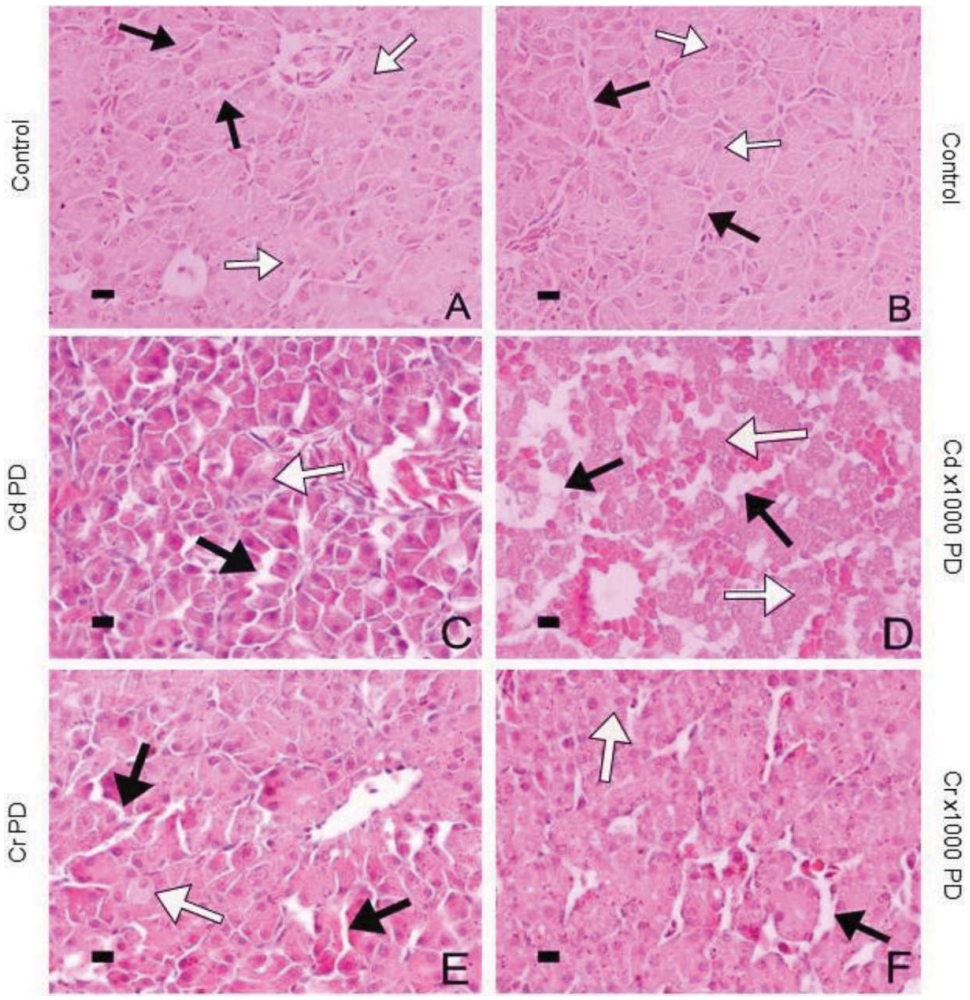

Fig. 1. Light microscopy micrographs of the liver tissue of the different experimental groups. A and B: control group. C and D: Cd PD and Cd ×1000 PD groups, E and F: Cr PD and Cr ×1000 PD groups. Black arrows indicate sinusoid dilation, white arrows in Figure A and B indicate the normal histology of the hepatocytes, whereas in Figures C-F the white arrows indicate cells undergoing necrosis (Scale bars: 10 μm).

sinusoids (black arrows). Figures 1C and D are representative of embryos exposed to the PD of Cd and ×1000 PD respectively. Minimal sinusoidal dilation is visible in the Cd PD group (indicated in Figure 1C), with a noticeable increase in sinusoidal dilation in the Cd ×1000 PD group (Fig. 1D) (black arrows). Some necrosis is also visible in both Cd concentration groups indicated by the white arrows in Figures 1C and 1D. This was not observed in the control group. The same pattern can be seen in the groups exposed to Cr as indicated in Figures 1E and 1F, but with less severity. In both Figures 1E and 1F the black arrows indicate sinusoidal dilation and the white arrows indicate necrosis of the hepatocytes.

Representative TEM micrographs of the liver tissue from the control and Cd experimental groups are shown in Figure 2. A hepatocyte, typical of the control samples, is shown in Figures 2A and 2B with normal cellular [Fig. 2A (black arrows)] and nuclear double membranes and evenly dispersed chromatin [Fig. 2A (white arrow)]. The mitochondria displayed a typical round or oval shape, with a double membrane that surrounds the cristae of the mito-

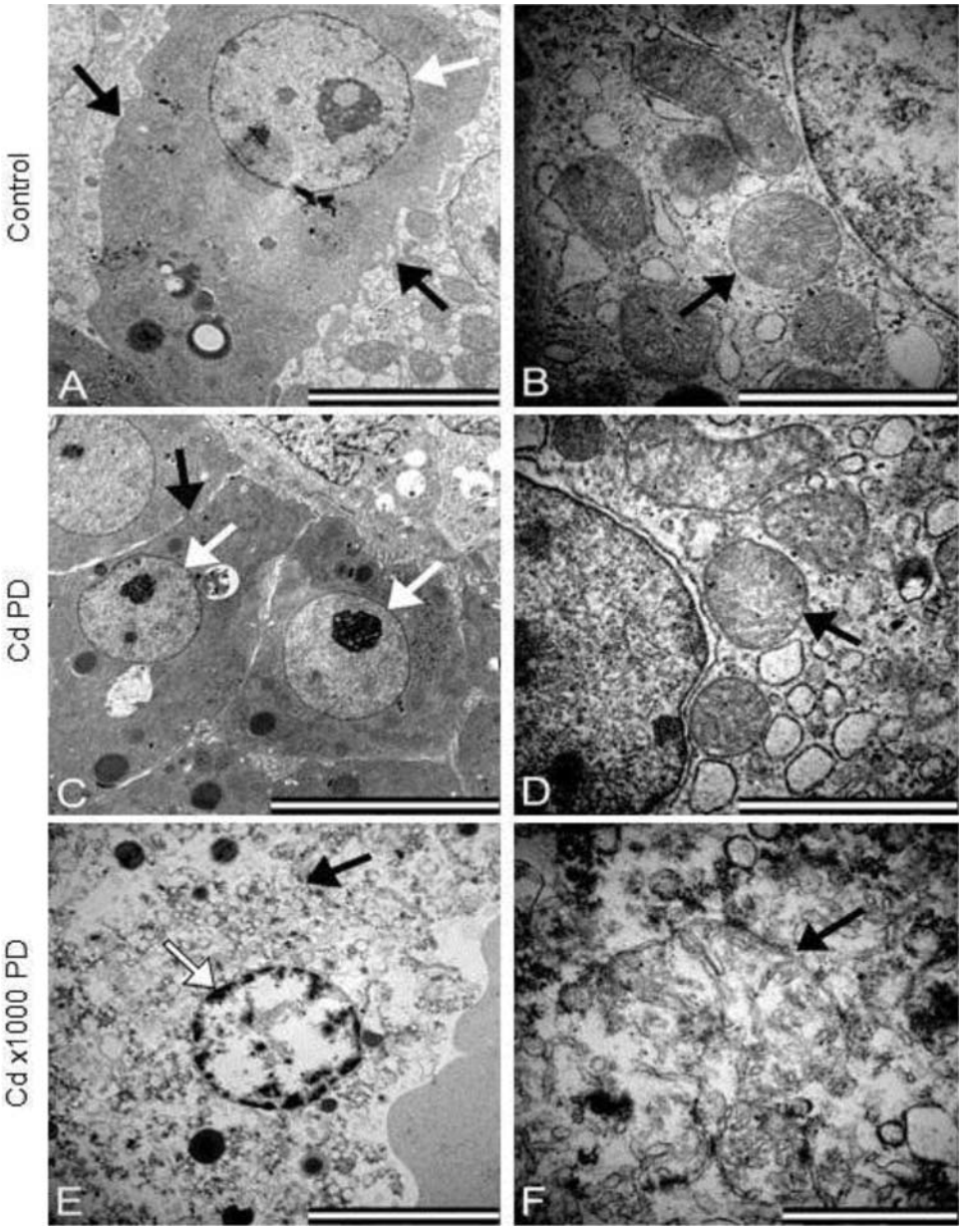

Fig. 2. Transmission electron micrographs of the hepatocytes and mitochondria of the liver tissue from the control and the different Cd concentration groups. Figure A: control, C: Cd PD and E: Cd ×1000 PD. White arrows indicate the nuclei of the hepatocytes and the black arrows indicate the cellular membranes. Figures B, D and F indicate the mitochondrial morphology (black arrows) of the control (B), Cd PD (D) and Cd ×1000 PD (F) groups (Scale bars: A, C and E = 5 μm; B and D = 2 μm; F = 1 μm).

chondria [Fig. 2B (black arrow)]. In Figures 2C and 2D the hepatocytes of the Cd PD group revealed no significant variations compared to the control (Fig. 2A), with evenly dispersed nuclear chromatin, no mitochondrial damage [Fig. 2D (black arrow)] and intact nuclear [Fig. 2C (white arrows)] and cellular membranes [Fig. 2C (black arrows)]. Figures 2E and 2F are representative of the Cd ×1000 PD group where major alterations can be seen compared to the control group.

Figure 2E reveals major disruption of the typical hepatocyte morphology with irregular chromatin condensation [Fig. 2E (white arrow)], a ruptured cellular membrane [Fig. 2E (black arrow)] and damaged or absent organelles, as seen in Figure 2F that indicates an extensively damaged mitochondria (black arrow). Further evaluation with ESI micrographs identified the bio-accumulation of Cd in the nuclei of the hepatocytes (Fig. 3E). Figure 3A shows the Cd edge that was used in the EELS analysis, with Figures 3B–3D indicating the ESI micrographs of Cd in the nucleus of the hepatocyte at each specific edge that was analyzed. Figure 3E indicates the final Cd map, with the Cd in white.

In Figure 4, liver tissue from the Cr-exposed groups is shown and again compared to the same control micrograph as shown in Figure 2. The hepatocyte [Fig. 4C (black arrow)] and nuclear morphology [Fig. 4C (white arrow)] in the Cr PD group revealed no alterations, but the mitochondria [Fig. 4D (black arrow)] showed minimal mitochondrial inner matrix swelling. The Cr ×1000 PD group, shown in Figures 4E and 4F, respectively, are comparable to that of the control as little to no damage is observed with evenly spaced chromatin and intact cellular [Fig. 4E (black arrow)] and nuclear [Fig. 4E (white arrow)] membranes. Only slight damage to the mitochondrial membrane was observed [Fig. 4F (black arrows)]. EELS analysis of the mitochondria revealed the presence of Cr associated with the cristae as indicated in Figure 5E. Figure 5A shows the specific edges used in the EELS analysis, with Figures 5B—D indicating the ESI micrographs of Cr in the mitochondria of the hepatocyte at each specific edge that was analyzed. Figure 5E indicates the final Cr map, with the Cr in white.

Discussion

The primary effect of heavy metal toxicity is oxidative stress that causes reactive oxygen species (ROS), which affects essential functions of the membranes through lipid peroxidation, DNA oxidation and formation of protein aggregates.[17] In addition, heavy metals such as Cd and Cr may also have an effect on antioxidant elements such as glutathione reductase, glutathione peroxidase, superoxide dismutase and catalase.[18] Damage and loss of

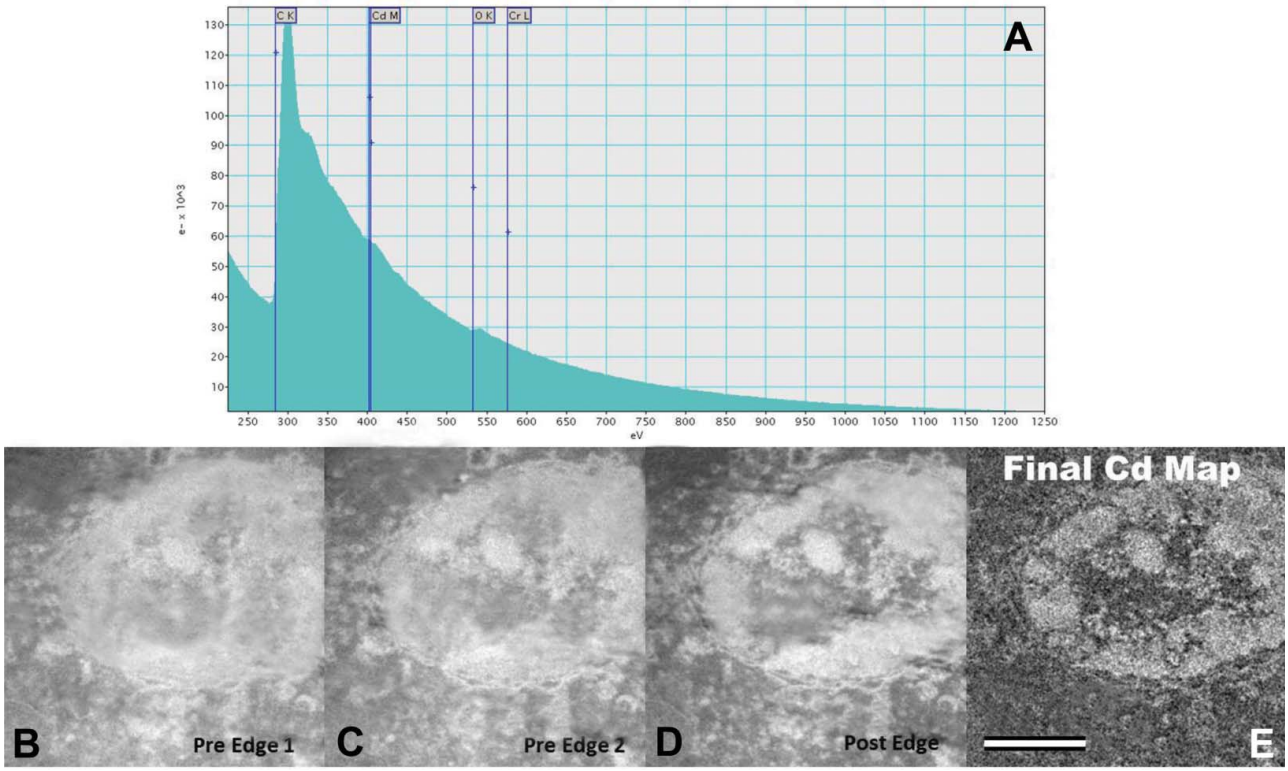

Fig. 3. EELS and ESI micrographs of liver tissue exposed to Cd ×1000 PD. Figure A shows the Cd edge that was used in the EELS analysis, with Figures B-D indicating the ESI micrographs of Cd in the nucleus of the hepatocyte at each specific edge that was analyzed. Figure E indicates the final Cd map, with the Cd in white (Scale bars: B, C, D and E: 1 μm).

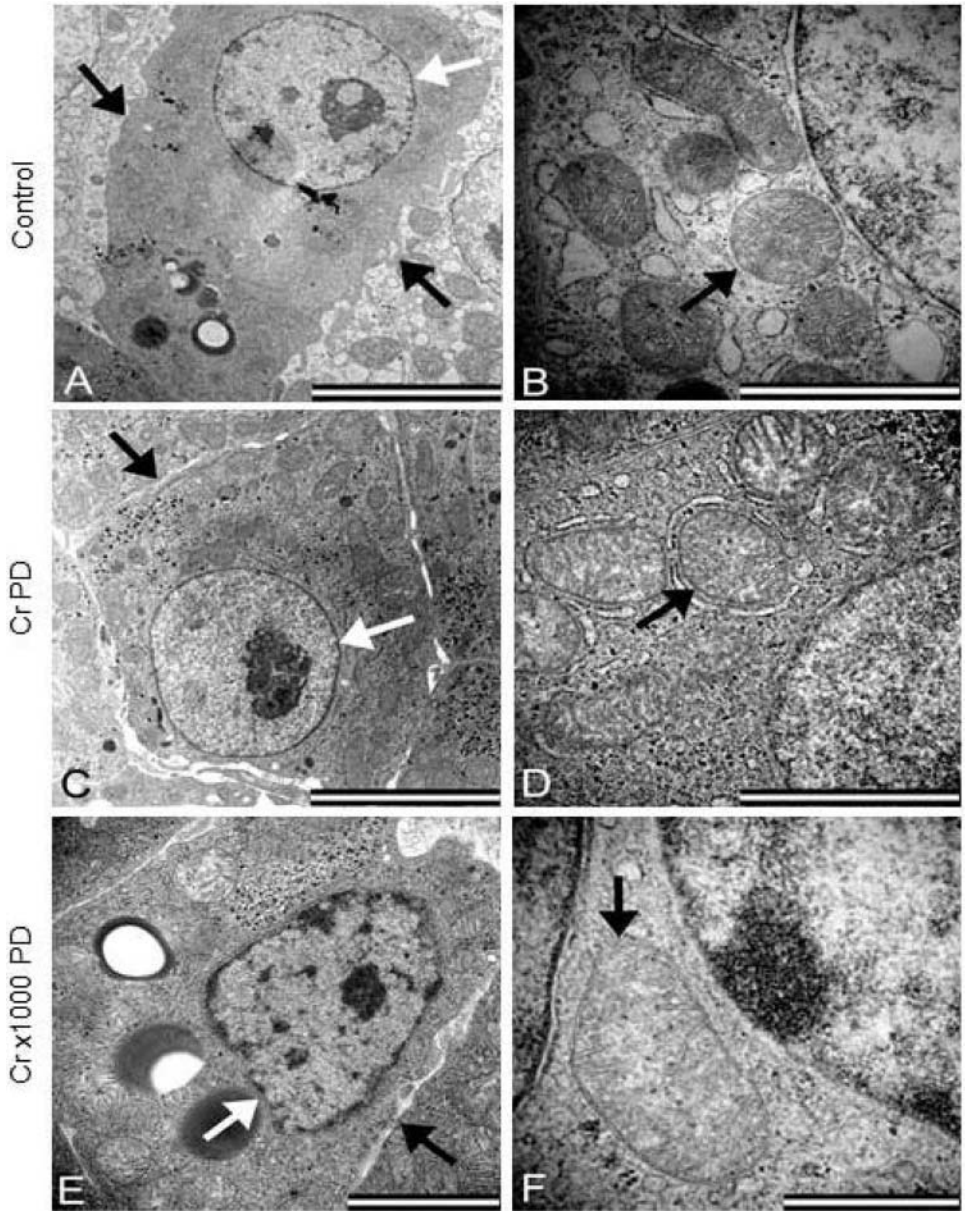

Fig. 4. Transmission electron micrographs of the hepatocytes and mitochondria of the liver tissue of the control and different Cr experimental groups. Figure A: control, C: Cr PD and E: Cr ×1000 PD. The white arrows indicate the nuclei of the hepatocytes and the black arrows indicate cellular membranes. Figures B, D and F indicate the mitochondrial morphology (black arrows) of the control, Cr PD and Cr ×1000 PD groups respectively (Scale bars: A and C = 5 μm; B, D and E = 2 μm; F = 1 μm).

essential function and/or depletion of antioxidant elements can lead to apoptosis and necrosis.[17]

In this study, the effects of Cd and Cr on liver tissue were examined using light microscopy and TEM. Compared to the control, Cd and Cr at PD and ×1000 PD caused sinusoidal dilation and necrosis. Jihen et al. reported sinusoidal dilation and necrosis in rat liver tissue after Cd exposure.[19] Acharya et al. evaluated the effects of Cr on rats and found that Cr caused an increase in sinusoidal space, vacuolation and necrosis in the liver tissue of these animals.[20] These studies differ in the animal model, dosage and concentrations of the metals used, however it is clear from this study that in the *in ovo* model, Cd and Cr are absorbed and cause significant hepatic damage in the developing embryo.

Evaluation of hepatocyte morphology at an ultrastructural level revealed no observable differences between the PD groups compared to the controls, and hepatocytes in both groups had evenly dispersed chromatin and no nuclear or cellular membrane damage. In contrast, in the

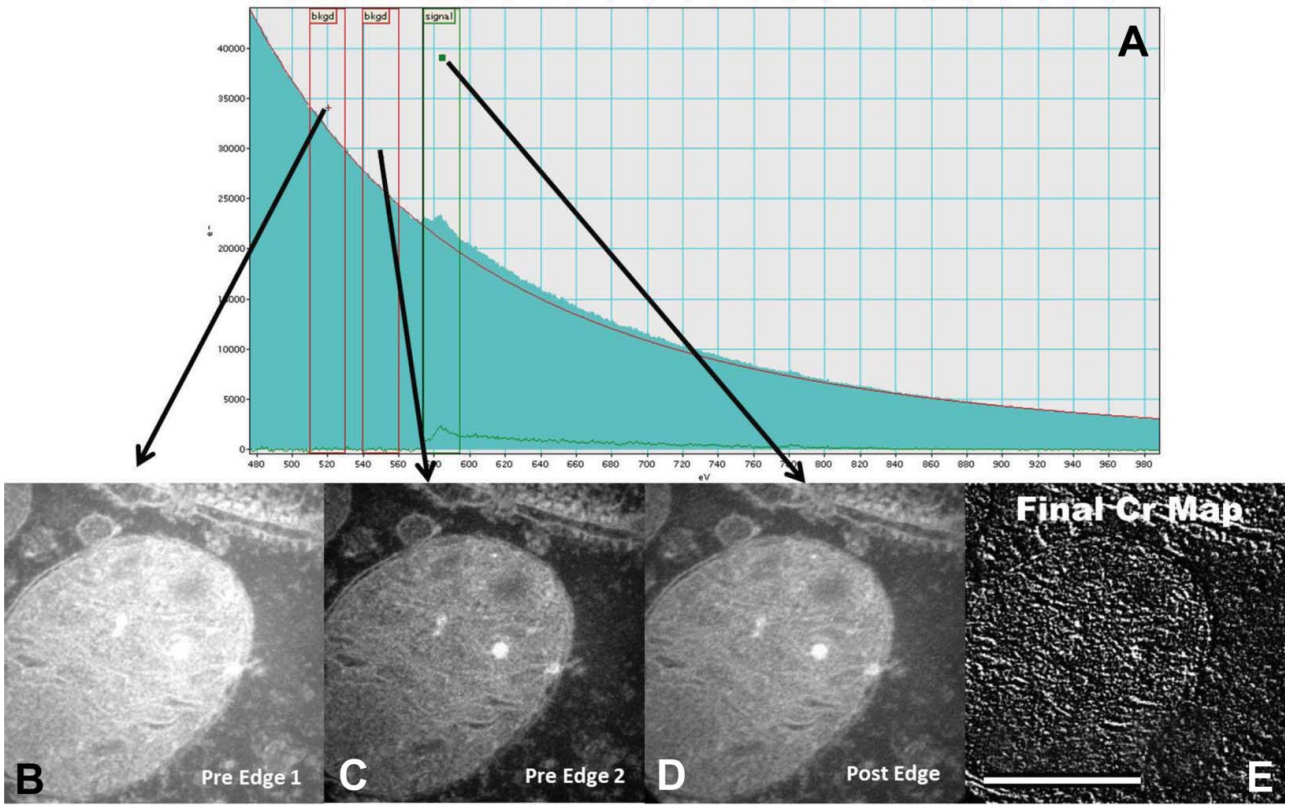

Fig. 5. EELS and ESI micrographs of liver tissue exposed to Cr ×1000 PD. Figure A shows the specific edges used in the EELS analysis, with Figures B-D indicating the ESI micrographs of Cr in the mitochondria of the hepatocyte at each specific edge that was analyzed. Figure E indicates the final Cr map, with the Cr in white (Scale bars: B, C, D and E: 0.5 μm).

×1000 PD groups, especially in the Cd ×1000 PD group, severe cellular damage was observed. Damage to the cell membrane, irregular chromatin condensation and mitochondrial damage was observed.

In 2000, Karmakar et al. investigated the effects of Cd exposure on the liver tissue of male Balb/c mice using light microscopy and TEM. The mice were exposed for 7, 14 and 21 days. At day 21, light microscopy revealed altered tissue morphology of the liver. Further TEM analysis revealed changes in the nuclei and mitochondria of the hepatocytes.[21] Similar structural changes in the morphology of liver tissue were found in mice exposed to Cr. In this study, Wang and colleagues, exposed mice to Cr and found that Cr can induce dose- and time-dependent DNA damage, hepatic oxidative stress and apoptosis in the hepatocytes.[22]

Increased levels of ROS cause lipid peroxidation that results in changes in increased membrane fluidity, which brings about the efflux of cytoplasmic solutes and loss of membrane–protein activity.[17] Extensive lipid peroxidation causes total loss of membrane integrity, as observed in the Cd ×1000 PD group. In addition to oxidative damage, ROS can cause the carboxylation of protein, and ineffective proteosomal degradation can lead to the formation and accumulation of high molecular mass aggregates.[17] At equimolar concentrations, the ultrastructural effects of Cr were less than that of Cd; where for Cr the cell and nuclear membranes appeared to be intact, although some mitochondrial damage was observed. The reason for the more severe cellular damage observed in the Cd group may be due to the fact that Cr is naturally found in the body and is easily converted to a less toxic form by existing biochemical pathways.[16,23,24] Cd, on the other hand, is not naturally found in the body and thus the body needs to produce metallothionein to restrict the toxicity of Cd. During the production of metallothionein, Cd can damage the tissue, which may lead to altered liver and kidney functions.[15,25,26]

EELS analysis revealed bio-accumulation of the Cd and Cr in the nuclei and mitochondria of the hepatocytes. In two studies done by Lui and Kottke in 2003, the authors also found Cd and Cr present in the deposits of electron-dense granules in the nuclei and cell membranes of root cells after exposure to Cr for 1, 3 and 6 days and to Cd for 9 days.[27,28] Chemical quantification of Cd and Cr has shown that these metals accumulate in cells.[19,29] In contrast, EELS analysis identifies the intracellular sites of bio-accumulation and these specific sites are the nucleus and mitochondria as shown in Figures 3E and 5E for Cd and Cr respectively. Very little Cd is present in the cytoplasm

compared to that present in the nucleus. In the nucleus, Cd is present in the nuclear membrane and is also found with the chromatin. The effect of Cd on nuclear DNA is indirect, and increased oxidative stress is the result of Cd binding DNA amino bases and proteins, which can lead to direct DNA strand breaks and/or epigenetic changes.[30]

Membrane-associated mitochondrial complexes I and III are the major sites of intracellular ROS formation. Within the mitochondrial electron transport chain of complex I are several redox centers that can react with molecular oxygen, leading to the formation of the superoxide anion. This superoxide anion is released into the mitochondrial matrix and transformed into hydrogen peroxide either spontaneously or via manganese superoxide dismutase. The superoxide anion formed by complex III is also converted to hydrogen peroxide by Cu/Zn-dependent superoxide dismutase. The formation of water from hydrogen peroxide is catalyzed by catalase or glutathione peroxidase, or scavenged by mitochondrial thioredoxin, glutaredoxin as well as cytochrome *c*.[31] In the presence of excess reduced transition metals Fenton transformation occurs, which catalyzes the conversion of hydrogen peroxide to highly reactive hydroxyl ion and causes extensive damage to DNA, proteins and lipids. Both Cd and Cr were found to have accumulated very specifically along the cristae of the mitochondria as shown in Figure 5E for Cr. Associated along this membrane is complex I and III, the site where the superoxide anion is formed. Whether Cd and Cr directly bind to these proteins found in the cristae is unknown and is an important area of further research.

Conclusion

In conclusion Cd and Cr bio-accumulates in the mitochondria and nucleus of hepatocytes. At these sites both metals can cause DNA base modification, changes in cellular homeostasis and increased lipid peroxidation. The consequence of lipid peroxidation and DNA damage namely membrane damage and DNA condensation was observed for Cd while only mitochondria associated damage was observed for Cr.

Acknowledgments

The authors would like to thank Mr. Chris van der Merwe for his assistance with obtaining and analyzing the EELS results.

References

[1] Nordberg, G.F.; Fowler, B.A.; Nordberg, M.; Friberg, L.T. Introduction-General Considerations and International Perspectives. In *Handbook of Toxicology of Metal*; Nordberg, G.F.; Nogawa, K.; Nordberg, M.; Friberg, L.T., Eds.; Academic Press: Amsterdam and Boston, 2007a; 4–9.

[2] Al-Attar, A.M. Antioxidant effect of vitamin E treatment on some heavy metals-induced renal and testicular injuries in male mice. Saudi. J. Biol. Sci. **2011**, *18*, 63–72.

[3] Awofolu, O.R.; Mbolekwa, Z.; Mtshemla, V.; Fatoki, O.S. *Levels of trace metals in water and sediment from Tyume River and its effects on an irrigated farmland*, Water SA 31: South Africa, 2005; 87–94.

[4] Chowdhury, A.R. Recent Advances in Heavy Metals Induced Effect on Male Reproductive Function-A Retrospective. Med. Sci. **2009**, *2*(2), 37–42.

[5] Taylor, C.M.; Golding, J.; Emond, A.M. Lead, cadmium and mercury levels in pregnancy: the need for international consensus on levels of concern. Dev. Orig. Health. Dis. **2014**, *5*(1), 16–30.

[6] SouthAfrica.info. Available at http://www.southafrica.info (accessed May 2013).

[7] Binning, K.; Baird, D. *Survey of heavy metals in the sediments of the Swartkops River Estuary, Port Elizabeth South Africa*, Water SA: South Africa, 2001; *27*, 461–466.

[8] Naicker, K.; Cukrowska, E.; McCarthy, T.S. Acid mine drainage arising from gold mining activity in Johannesburg, South Africa and environs. Environ. Pollut. **2003**, *122*(1), 29–40.

[9] Fatoki, O.S.; Awofolu, R. *Levels of Cd, Hg and Zn in some surface waters from the Eastern Cape Province*, Water SA: South Africa, 2003; *29*, 375–380.

[10] Molokwane, P.E.; Meli, K.C.; Nkhalambayausi—Chirwa, E.M. Chromium (VI) reduction in activated sludge bacteria exposed to high chromium loading: Brits culture (South Africa). Water res. **2008**, *42*(17), 4538–4548.

[11] IOL Scitech. Witbank air dirtiest in the world. Available at http://www.iol.co.za/scitech/science/environment/(accessed Apr 2013)

[12] Gonzalez, P.; Baudrimont, M.; Boudou, A.; Bourdineaud, J.P. Comparative effects of direct cadmium contamination on gene expression in gills, liver, skeletal muscles and brain of the zebrafish (*Danio rerio*). BioMetals. **2006**, *19*(3), 225–235.

[13] Kuriwaki, J.I.; Nishijo, M.; Honda, R.; Tawara, K.; Nakagawa, H.; Nishijo H. Effects of cadmium exposure during pregnancy on trace elements in fetal rat liver and kidney. Toxicol. Lett. **2005**, *156*(3), 369–376.

[14] Robinson, J.; Avenant—Oldewage, A. *Chromium, copper, iron and magnesium bioaccumulation in some organs and tissue of Oreochromis mossambicus from the lower Olifants River, inside the Kruger National Park*, Water SA, **2006**; *23*, 387–403.

[15] Nordberg, G.F.; Nogawa, K.; Nordberg, M.; Friberg, L.T. Cadmium. In *Handbook of Toxicology of Metals*; Nordberg, G.F.; Nogawa, K.; Nordberg, M.; Friberg, L.T., Eds.; Academic Press: Amsterdam and Boston, 2007b; 445–486.

[16] Langård, S.; Costa, M. Chromium. In *Handbook on the Toxicology of Metal*; Nordberg, G.F., Fowler, B.A., Nordberg, M., Friberg, L.T., Eds. Academic Press: Amsterdam and Boston, 2007; 487–510.

[17] Avery, S.V. Molecular targets of oxidative stress. Biochem. **2011**, *434*, 201–210.

[18] Kim, S.H.; Jung, M.J.; Lee, Y.M. Effects of heavy metals on the antioxidant enzymes in the marine ciliate Euplotes Crassus. Toxicol. Environ. Health Sci. **2011**, *3*(4), 213–219.

[19] Jihen, E.H.; Imed, M.; Fatima, H.; Abdelhamid, K. Protective effects of selenium (Se) and zinc (Zn) on cadmium (Cd) toxicity in the liver and kidney of rats: Histology and Cd accumulation. Food. Chem. Toxicol. **2008**, *46*(11), 3522–3527.

[20] Acharya, S.; Mehta, K.; Krishnan, S.; Vaman Rao, C. A subtoxic interactive toxicity study of ethanol and chromium in male Wistar rat. Alcohol **2001**, *23*(2), 99–108.

[21] Karmakar, R.; Bhattacharya, R.; Chatterjee, M. Biochemical, haematological and histopathological study in relation to time-related cadmium-induced hepatotoxicity in mice. BioMetals **2000**, *13*(3), 231–239.

[22] Wang, X.F.; Xing, M.L.; Shen, Y.; Zhu, X.; Xu, L.H. Oral administration of Cr(VI) induced oxidative stress, DNA damage and apoptosis cell death in mice. Toxicology **2006**, *228*(1), 16–23.
[23] Dayan, A.D.; Paine, A.J. Mechanisms of chromium toxicity, carcinogenicity and allergenicity: Review of the literature from 1985 to 2000. Hum. Exp. Toxicol. **2001**, *20*(9), 439–451.
[24] Raghunathan, V.K.; Ellis, E.M.; Grant, M.H. Response to chronic exposure to hexavalent chromium in human monocytes. Toxicol. in Vitro **2009**, *23*(4), 647–652.
[25] Prozialeck, W.C.; Edwards, J.R.; Woods, J.M. The vascular endothelium as a target of cadmium toxicity. Life. Sci. **2006**, *79*(16), 1493–1506.
[26] Valko, M.; Rhodes, C.J.; Moncola, J.; Izakovic, M.; Mazura, M. Free radicals, metals and antioxidants in oxidative stress-induced cancer. Chem. Biol. Interact. **2006**, *160*(1), 1–40.
[27] Lui, D.; Kottke, I. Subcellular localization of Cd in the root cells of Allium sativum by electron energy loss spectroscopy. J. Biosci. **2003a**, *28*(4), 471–478.
[28] Lui, D.; Kottke I. Subcellular localization of chromium and nickel in root cells of *Allium cepa* by EELS and ESI. Cell. Biol. Toxicol. **2003b**, *19*(5), 299–311.
[29] Krumschnable, G.; Nawaz, M. Acute toxicity of hexavalent chromium in isolated teleost hepatocytes. Aquat. Toxicol. **2004**, *70*(2), 159–167.
[30] Ray, D.R.; Yonsim, A.; Fry, R.C. Incorporating epigenetic data into the risk assessment progress for the toxic metal arsenic, cadmium, chromium, lead and mercury; strategies and challenges. Front. Genet. **2014**, *5*, 1–26.
[31] Moreira, A.C.; Machando, N.G.; Bernardo, T.C.; Sardão, V. A.; Oliveira, P.J. Mitochondria as a biosensor for drug-induced toxicity – Is really relevant? InTech. **2011**, *4*(1), 411–444.